ELEMENTA
Science of the Anthropocene

Lukovich, JV, et al. 2021. A baseline evaluation of atmospheric and river discharge conditions in the Hudson Bay Complex during 2016–2018. *Elem Sci Anth*, 9: 1. DOI: https://doi.org/10.1525/elementa.2020.00126

RESEARCH ARTICLE

A baseline evaluation of atmospheric and river discharge conditions in the Hudson Bay Complex during 2016—2018

Jennifer V. Lukovich[1,*], Andrew Tefs[2], Shabnam Jafarikhasragh[1], Clark Pennelly[3], Paul G. Myers[3], Tricia A. Stadnyk[2], Kevin Sydor[4], Karen Wong[4], Michael Vieira[4], David Landry[1], Julienne C. Stroeve[1,5,6], and D. G. Barber[1]

In this article, we examine atmospheric and river discharge conditions within the Hudson Bay Complex for the BaySys 2016–2018 field program time frame. Investigated in particular is a subset of European Centre for Medium-Range Weather Forecasts (ECMWF) Re-Analysis - Interim (ERA-Interim) atmospheric forcing variables, namely 2-m surface temperature, 10-m surface winds, precipitation, and sea-level pressure, in addition to river discharge. Results from this assessment show that 2016 was characterized by unusually warm conditions (terrestrial and marine) throughout the annual cycle; 2017 by strong cyclone activity in March and high precipitation in January, October, and November; and 2018 by cold and windy conditions throughout the annual cycle. Evaluation of terrestrial conditions showed higher than normal land surface temperatures (the Hudson Bay physical watershed) for all of the 2016–2018 period (excluding a colder than normal spell August–November 2018), particularly in January (2016 and 2017), higher than normal precipitation in October (2016 and 2017), and higher than normal terrestrial discharge to the Hudson Bay Complex in March (2016 and 2017), with drier than average June through October (2016–2018).

Keywords: Atmospheric conditions, River discharge conditions, Baseline evaluation for 2016–2018, BaySys, Hudson Bay Complex, Standardized anomalies and rankings

1. Introduction

Hudson Bay is an inland sea and gateway between North America and the rest of the world. It acts as a conduit between the Arctic and midlatitude regions, as well as the Canadian rivers that comprise its watershed and the Atlantic Ocean. Hudson Bay (HB) further provides a signature of freshwater–marine coupling, as well as local and global effects and interactions from the perspective of science and society.

From the arrival of the English ship the *Nonsuch* in Hudson Bay in 1668 that launched the fur trade in North America and connections between Indigenous and European communities, to centuries of exploration and scientific discovery under the auspices of the Hudson's Bay Company, through to Canadian Confederation in 1867, construction of the Hudson Bay railway line in 1920 and more recently hydroelectric development in the 1960s, Hudson Bay and its communities have witnessed the impacts of altered landscapes due to human interventions such as river discharge regulation, and a changing climate.

In 2014, a collaboration between Manitoba Hydro, the Universities of Manitoba, Alberta, Laval, and Ouranos began in an attempt to characterize the latter impacts. As outlined in the Preface and Introduction to this special collection, the Hudson Bay System Study (BaySys) is a collaborative project focused on relative climate change and river discharge regulation (hereinafter referred to as regulation) impacts on freshwater–marine coupling in the Hudson Bay Complex (HBC). BaySys consisted of six teams to study the marine and climate system, freshwater and littoral system, marine ecosystem, carbon cycling, contaminants and their simulated representation in the HBC. The observational component included a series of field campaigns conducted onshore and onboard the icebreaker the Amundsen to characterize marine and estuarine physical and biogeochemical processes during the

[1] Centre for Earth Observation Science, University of Manitoba, Winnipeg, MB, Canada
[2] Department of Geography, University of Calgary, Calgary, AB, Canada
[3] Department of Earth and Atmospheric Sciences, University of Alberta, Edmonton, AB, Canada
[4] Manitoba Hydro, Winnipeg, MB, Canada
[5] Centre for Polar Observation and Modelling, Earth Sciences, University College London, London, UK
[6] National Snow and Ice Data Centre, University of Colorado, Boulder, CO, USA

* Corresponding author:
Email: Jennifer.Lukovich@umanitoba.ca

2016–2018 time frame. The modeling component included the Arctic and Northern Hemisphere Atlantic (ANHA) configuration, developed at the University of Alberta, of the Nucleus for European Modeling of the Ocean–Louvain-la-Neuve sea Ice Model, Version 2 (NEMO-LIM2) ice-ocean model (Version 3.6), which takes as "input" atmospheric forcing variables and river discharge, and generates as "output" ice and oceanographic variables relevant to all BaySys teams for an evaluation of relative and combined climate change and freshwater regulation impacts on physical and biogeochemical processes in the HBC.

This paper and the companion paper (Lukovich et al., n.d.) provide a baseline evaluation of atmospheric, discharge, and sea ice conditions in the HBC during the 2016–2018 BaySys time frame. This study aims to provide context of present-day atmospheric and river discharge changes relative to the 1981–2010 climatology. Examined in particular is sea-level pressure (SLP) to provide a regional characterization of atmospheric circulation. Also examined are surface (10 m) wind speed, surface (2 m) temperature, and total precipitation (rainfall and snowfall), in addition to river discharge, terrestrial temperature, and total precipitation to characterize local conditions. The companion paper examines oceanographic and sea ice conditions in the HBC for the BaySys time frame (Lukovich et al., n.d.).

Previous studies have examined river discharge, atmospheric, oceanic, and sea ice conditions in the HBC from both an observational and a modeling perspective (Maxwell, 1986; Prinsenberg, 1986a, 1986b; Prinsenberg, 1987; Saucier et al., 2004; Gagnon and Gough, 2005; Hochheim and Barber, 2010; Déry et al., 2011; Déry et al., 2018; Hochheim et al., 2011; Landy et al., 2017; Jafarikhasragh et al., 2019; Ridenour et al., 2019; Kirillov et al., 2020). In winter, large-scale atmospheric circulation is characterized by the Aleutian and Icelandic lows in the northern Pacific and Atlantic sectors and in Hudson Bay by gradients established between an SLP high in the Mackenzie region and SLP low in the vicinity of Baffin Bay, variations in upper level winds that induce a poleward migration in storms, and storms from the Labrador coast. In summer, large-scale circulation is characterized by SLP high regimes over midlatitude Pacific and Atlantic regions and in Hudson Bay by the migration of SLP lows into the region that contribute to enhanced variability in local circulation patterns. Atmospheric conditions within HB are influenced by the tropopause polar vortex (TPV; Cavallo and Hakim, 2010). During winter, the TPV over northern Baffin Bay results in north-westerly winds in western HBC and south-westerly winds in eastern Hudson Bay (Maxwell, 1986). In summer, atmospheric conditions are governed by a poleward retreat of the TPV, and winds switch to westerly over Hudson Bay.

Regional-scale changes in atmospheric patterns and the location and strength of the TPV also influence ice and oceanic conditions, examined by Lukovich et al. (n.d.). In particular, the North Atlantic Oscillation (NAO) and El Nino influence sea ice concentration (Mysak et al., 1996), while wind stress influences sea ice drift. Recent studies have also highlighted the role of the Arctic Oscillation, an Arctic-focused expression of the NAO, in driving sea ice variability (Proshutinsky et al., 2015). The seasonal impact of atmospheric forcing on ice conditions is demonstrated in Hochheim et al. (2011) where sea ice extent in Hudson Bay in spring is shown to be governed by local atmospheric processes, in contrast to fall, where sea ice conditions are governed by the nonlocal East Pacific/North Pacific atmospheric patterns. These results are further corroborated in a recent study demonstrating atmospheric vorticity impacts on oceanographic rather than ice conditions, where northerly atmospheric flow induces Ekman transport and onshore transport and downwelling (Dmitrenko et al., 2020), presented in this special issue. On the other hand, regional changes in snow and sea ice also feedback on atmospheric circulation (e.g., Walsh, 2014; Screen, 2017), as well as the position of the Arctic Frontal Zone, a region of steep temperature gradients that plays a role in intensifying cyclones that migrate across the Arctic coast (Crawford and Serreze, 2016).

In addition to atmospheric forcing, river discharge influences marine conditions in Hudson Bay. River discharge to the HBC is affected by anthropogenic influences and human intervention including diversions, dams, and reservoirs. The Hudson Bay Watershed (HBW) encompasses five Canadian provinces (Quebec, Ontario, Manitoba, Saskatchewan, and Alberta), two territories (Nunavut and the Northwest Territories), and four American states (North and South Dakota, Minnesota, and Montana). Dominant rivers include the Nelson, Churchill, La Grande, and Saskatchewan Rivers; key waterbodies include Lake Winnipeg, Lake Manitoba, and Lake of the Woods. The Churchill River was diverted into the Nelson River to increase flow by 40% in 1976. The Churchill and Nelson Rivers support six hydroelectric stations in the lower Nelson River. The diversion of the Eastmain River and the portion of the Koksoak River upstream of Caniapiscau Lake to the La Grande River in 1980 and 1982, respectively, resulted in a near doubling of discharge (Déry et al., 2011; Déry et al., 2018). In 2009, diversion of the Rupert River further increased the La Grande discharge. Based on the degree to which the natural flow regime is disrupted (regulation) and the number of control points along their river courses (fragmentation), the Nelson and La Grande watersheds are classified as "severely" regulated and fragmented by the indices outlined by Grill et al. (2015). A mean annual discharge of 122 km^3y^{-1} in the Churchill and Nelson Rivers and 121 km^3y^{-1} for the La Grande, Eastmain, and Rupert Rivers have been previously reported over the period 1964–2013 (Déry et al., 2016). Nearshore processes are impacted by regulation via changes to density and salinity; offshore impacts remain poorly understood (Stewart and Lockhart, 2005). Regulation also influences the seasonality of discharge, with implications for circulation and ice conditions within Hudson Bay. Higher streamflow during colder winter months favors sea ice formation due to freshening of surface waters (Ingram and Prinsenberg, 1998; Saucier et al., 2004) and through the extension of under-ice plumes (Whittaker, 2006). Approximately 30% of gauged area in the HBW landmass is unregulated (Déry et al., 2011), with the five largest

unregulated rivers (confluence of Thelon and Kazan rivers that comprise the Chesterfield Inlet river system, Nottaway River, George River, Severn River, and Hayes River) generating natural average annual discharge of 138 km^3y^{-1} over the same period (Déry et al., 2016).

This article is intended to provide a baseline understanding of the observation period (2016–2018) compared to the longer 1981–2010 historical record in the region. Spatial variability in atmospheric variables is captured in monthly standardized anomaly maps (presented as Supplementary Material). Temporal variability is captured in time series for spatially averaged variables. Relative contributions of atmospheric and discharge variables to freshwater–marine coupling and ice-ocean processes are presented in the context of rankings as a function of variable and year.

This baseline evaluation is structured as follows. Data and the definition used in this study for standardized anomalies are presented in Section 2. Temporal and spatial variability are presented in Section 3.1 in monthly plots or "heat maps" of atmospheric and river discharge spatially (area-weighted) averaged over both the HBC and watershed, and time series. Also included in this section is a description of spatial variability in atmospheric and discharge conditions documented in the Supplemental Material in standardized anomaly maps of SLP, 10-m wind speeds, surface temperature (terrestrial and marine), precipitation (terrestrial and marine), and river discharge. Relative contributions of atmospheric and discharge conditions to freshwater–marine processes are presented based on rankings of spatially averaged variable values and their standardized anomalies in Section 3.2. The same analysis for atmospheric conditions is repeated and presented in Section 3.3 for the HBW, to illustrate regional, or nonlocal, contributions. Section 4 provides a synopsis of results from the atmospheric and river discharge baseline evaluation in the HBC during the 2016–2018 BaySys time frame.

2. Data and methods

Atmospheric conditions are investigated using European Centre for Medium-Range Weather Forecasts (ECMWF) Re-Analysis - Interim (ERA-Interim), available from 1979 to the end of 2019, with a horizontal spatial resolution of approximately 0.7° (Dee et al., 2011). ERA-Interim includes an atmospheric model and data assimilation system that provides an improved representation of the hydrological cycle and stratospheric processes as compared to its earlier version, ERA-40. Strengths of ERA-Interim include the availability of multiple atmospheric variables with high spatial resolution and temporal frequency produced within a consistent framework; weaknesses associated with water cycling intensity over oceans and boundary layer processes are addressed in a more recent version, ERA5, which was unavailable at the time of analyses presented in this article. In this study, ERA-Interim reanalysis data including mean SLP, zonal (u), and meridional (v) surface (10 m) wind components used to compute surface wind speeds ($\sqrt{u^2 + v^2}$), surface (2 m) temperature, and precipitation are evaluated for the 2016–2018 BaySys time frame relative to the 1981–2010 climatology.

Terrestrial (overland) precipitation and temperature, used as input to the BaySys Team 2 Hudson-HYdrological Predictions for the Environment (H-HYPE; Andersson et al., 2015; Stadnyk et al., 2020) hydrological model, are investigated using the Hydrological Global Forcing Data product (HydroGFDv2, 0.5° grid; Berg et al., 2018) over the HBW. HydroGFD is an updated and extended version of the Watch Forcing Data-ERA-Interim method; although both use ERA-Interim, HydroGFD enables other reanalysis products to replace the ERA-Interim reanalysis to allow for correction in bias in temperature and precipitation. Modeled discharge from all outlets in the H-HYPE model were, in addition to the ERA-Interim atmospheric forcing variables, used as input to the ANHA configuration of the NEMO ice-ocean model. Subbasin discharge is derived from all subbasins in H-HYPE for spatial analyses and presented as the sum of all modelled outlets to the HBC (398 discrete watersheds from 6,668 subbasins) for time series and temporal ranking analyses. H-HYPE subbasins are delineated based on topography and HydroGFD is downscaled to the subbasin polygons based on the areas where grid cells overlap those polygons (using an area weighting, or Thiessen polygon type analysis). Monthly results are presented here from 1981 to 2018, modeled on a daily time step.

It should be noted that the correlation coefficients for HydroGFD and ERA-Interim HBW monthly precipitation and temperature are 0.691 and 0.998, respectively, for the 1981–2010 time frame. Correlation coefficients for the HydroGFD and ERA-Interim precipitation standardized anomalies are 0.70, 0.87, and 0.50, and for temperature standardized anomalies are 0.85, 0.88, and 0.91 for 2016, 2017, and 2018, respectively. Weaker correlations between the overland and reanalysis precipitation standardized anomalies may be attributed to regional variability and spatial correlations over smaller spatial scales for precipitation as compared to temperature.

Standardized anomalies are computed based on the relation

$$x_a = \frac{x - \mu}{\sigma},$$

where x_a is the standardized anomaly for the atmospheric and discharge variable of interest x, μ is the mean climatology for the 1981–2010 time frame, and σ is the standard deviation, each computed separately for each calendar month in the 1981–2010 time frame. The standardized anomaly, as the ratio of the variable anomaly to its standard deviation, is a unitless entity. The temporal (1981–2010) mean is computed for standardized anomaly maps, and spatiotemporal (1981–2010 climatology, latitude and longitude) mean for standardized anomaly time series. Standardized anomalies are computed to eliminate seasonal features and climatological variance, as noted in Dabernig et al. (2017), and thus provide a consistent framework for comparison among the atmospheric and discharge forcing variables. Standard deviation maps for the 1981–2010 climatology are also provided in the Supplemental Material section for reference.

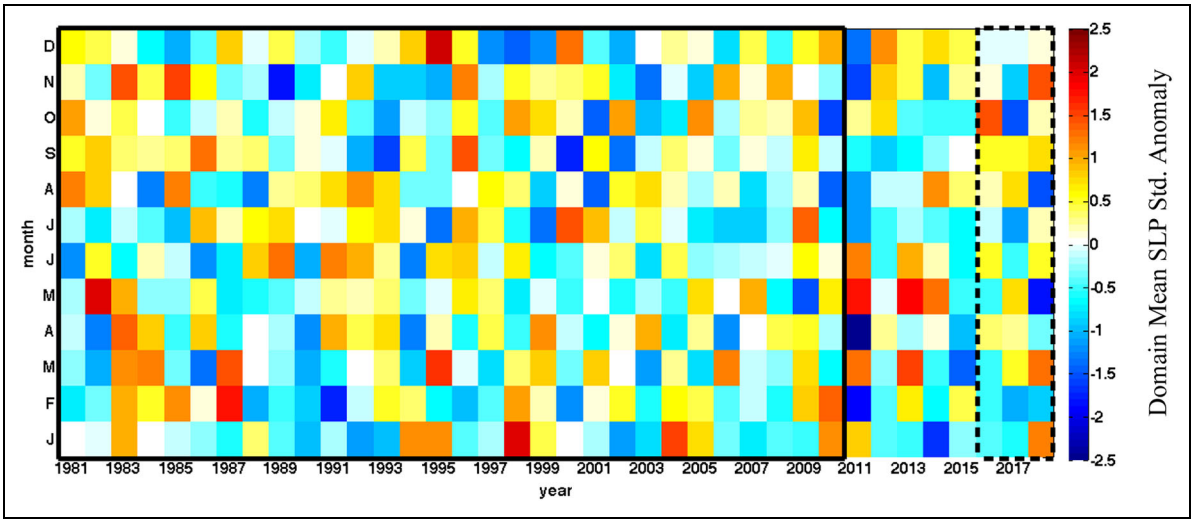

Figure 1. Monthly ERA-Interim sea-level pressure (SLP) standardized anomalies from 1979 to 2018. Month–year plots of mean ERA-Interim SLP standardized anomalies spatially averaged over the Hudson Bay Complex, with red (blue) indicating SLP high (low) regimes. The solid rectangle perimeter depicts the 1981–2010 climatology, and the dashed rectangle perimeter the 2016–2018 BaySys time frame. Standardized anomalies refer in this and subsequent figures to the ratio in the variable anomalies to their standard deviations with respect to the 1981–2010 climatology, and are unitless. ERA-Interim = European Centre for Medium-Range Weather Forecasts (ECMWF) Re-Analysis - Interim. DOI: https://doi.org/10.1525/elementa.2020.00126.f1

Year–month plots and time series are provided for values spatially averaged (and weighted by latitude) over the HBC ([100°W, 70°W; 50°N, 70°N]; main section) and HBW ([120°W, 60°W; 42°N, 75°N]; Supplemental Material section) to allow for comparison of conditions at local and regional scales, respectively. Terrestrial variables (reanalysis temperature and precipitation, as well as modeled discharge) are spatially averaged over those sections of the HBW that make up the physical watershed. In addition, the interquartile range (IQR) of values within the region of interest (HBC, HBW) is presented for time series to account for spatial variability in each variable.

In order to quantify relative contributions from atmospheric and discharge conditions to freshwater–marine coupling in the HBC and HBW from 2016 to 2018, spatially averaged values for each month and season are sorted, or ranked, in ascending order. The equations used in the spatiotemporal analysis of atmospheric and river discharge variables are presented at the end of the Supplementary Material, for reference.

3. Results

3.1. Temporal and spatial variability in atmospheric and discharge conditions

3.1.1. Atmospheric conditions

Monthly plots and time series of SLP, surface winds, surface temperature, and precipitation and their standardized anomalies illustrate temporal variability and differences between years during the 2016–2018 time frame. Anomalies are computed relative to 1981–2010. This period was selected since it (1) is postregulation and (2) coincides with an Environment and Climate Change Canada climatological and conventional normal time interval. Postregulation in this case includes the development of run-of-the-river hydroelectric generation on the Albany and Moose Rivers; diversion of the Churchill River into the Nelson River; diversion of the Eastmain, Opinaca, and Caniapiscau Rivers to the La Grande River; and hydroelectric impoundment and regulation of the Nelson and La Grande Rivers. It includes only 1 year of the Rupert River diversion, which is fully in effect by 2016–2018.

Monthly SLP standardized anomalies (**Figure 1**) during the BaySys 2016–2018 time frame illustrate contrasting SLP low and high regimes in January, 2017 and 2018; May, 2017 and 2018; August, 2017 and 2018; and October, 2016 and 2017. These contrasting regimes coincide in January with negative SLP anomalies in southwestern HB in 2017 and positive SLP anomalies in southeastern and central HB in 2018. In May, positive SLP anomalies are observed in 2017 and negative anomalies in 2018 over Hudson Strait. In August, negative anomalies exist throughout HBC in 2017, while positive anomalies exist in northeastern HBC in 2018. Contrasting regimes are further evidenced in October in positive SLP anomalies over central and to the northwest of HB in 2016, and negative anomalies to the southwest of HB in 2017 (Supplemental Figures S1A–S1C). Noteworthy also is the negative anomaly located in the vicinity of the Port of Churchill in March 2017 associated with the SLP low and March blizzard.

Surface wind speed standardized anomalies (**Figure 2**) show contrasting wind regimes in February, May, and August, with comparatively calm conditions in 2017, and windy conditions in 2018. In February, these correspond spatially to negative anomalies characteristic of weak winds in northern and southern HB in 2017, and a steep gradient between weak and strong winds over northwest HB in 2018. In May, calm conditions are observed over central and northern HB in 2017, while windy conditions

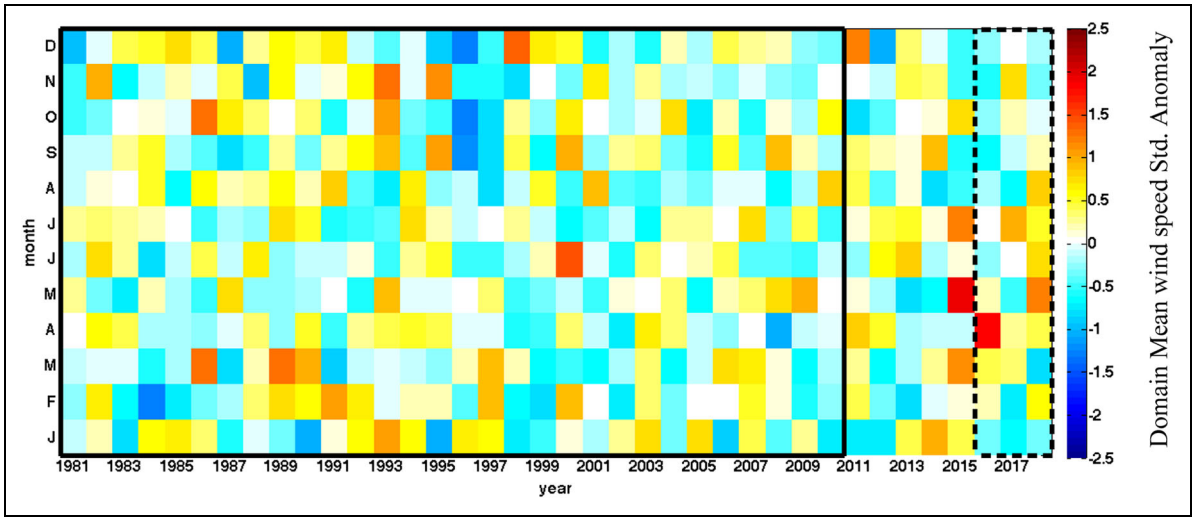

Figure 2. Monthly ERA-Interim surface winds speed standardized anomalies from 1979 to 2018. Month–year plots of mean ERA-Interim surface wind speed standardized anomalies spatially averaged over the Hudson Bay Complex, with red/blue shading indicating high/low wind regimes. Surface wind speeds are computed from ERA-Interim zonal (u) and meridional (v) surface wind components as $\sqrt{u^2 + v^2}$. The solid rectangle perimeter depicts the 1981–2010 climatology, and the dashed rectangle perimeter the 2016–2018 BaySys time frame. Standardized anomalies, as the ratio in surface wind anomalies and their standard deviations with respect to the 1981–2010 climatology, are unitless. ERA-Interim = European Centre for Medium-Range Weather Forecasts (ECMWF) Re-Analysis - Interim. DOI: https://doi.org/10.1525/elementa.2020.00126.f2

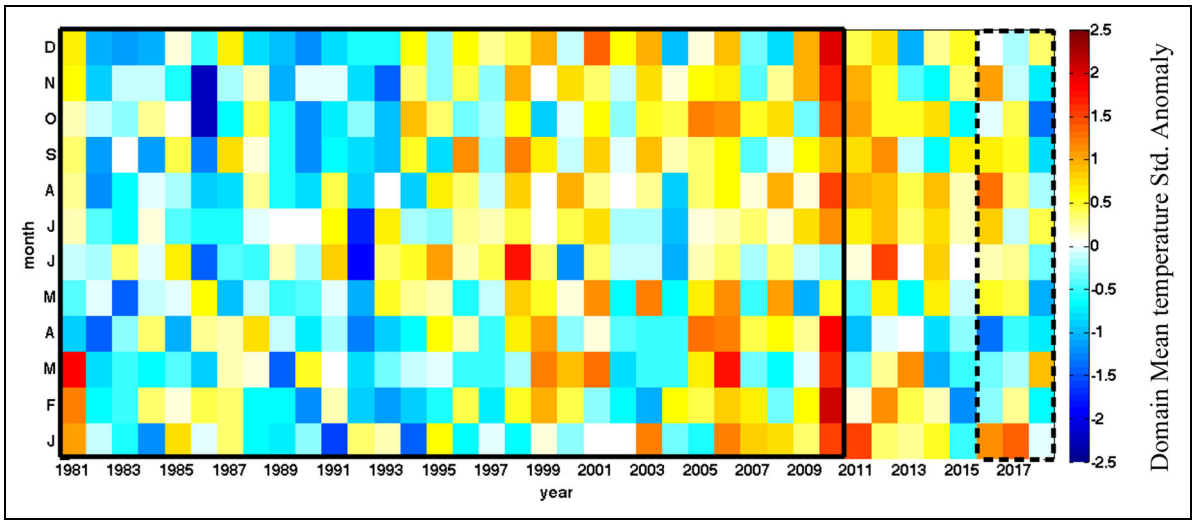

Figure 3. Monthly ERA-Interim surface temperature standardized anomalies from 1979 to 2018. Month–year plots of mean ERA-Interim surface temperature standardized anomalies spatially averaged over the Hudson Bay Complex, with red (blue) shading indicating high (low) temperature regimes. The solid rectangle perimeter depicts the 1981–2010 climatology, and the dashed rectangle perimeter the 2016–2018 BaySys time frame. Standardized anomalies are unitless. ERA-Interim = European Centre for Medium-Range Weather Forecasts (ECMWF) Re-Analysis - Interim. DOI: https://doi.org/10.1525/elementa.2020.00126.f3

are observed over northern, and to the east of, HB in 2018. In August, calm (windy) conditions are observed throughout the HBC in 2017 (2018; Supplemental Figures S2A–S2C). A sharp gradient in high winds along the western coast of HB and weaker winds over central HB provides a signature of the aforementioned blizzard in March 2017 in contrast to predominantly weak winds and calm conditions in 2018. Unusually strong winds in April 2016 depict the strong SLP gradient between an anomalous SLP low over Baffin Bay and SLP high over the Mackenzie Basin reported at this time (National Snow and Ice Data Centre Arctic Sea Ice News & Analysis, 2016, and Supplemental Figure S1A) that gives rise to high winds in this region, as documented by Maxwell (1986).

Corresponding surface temperature standardized anomalies (**Figure 3**) capture comparatively warm (cold)

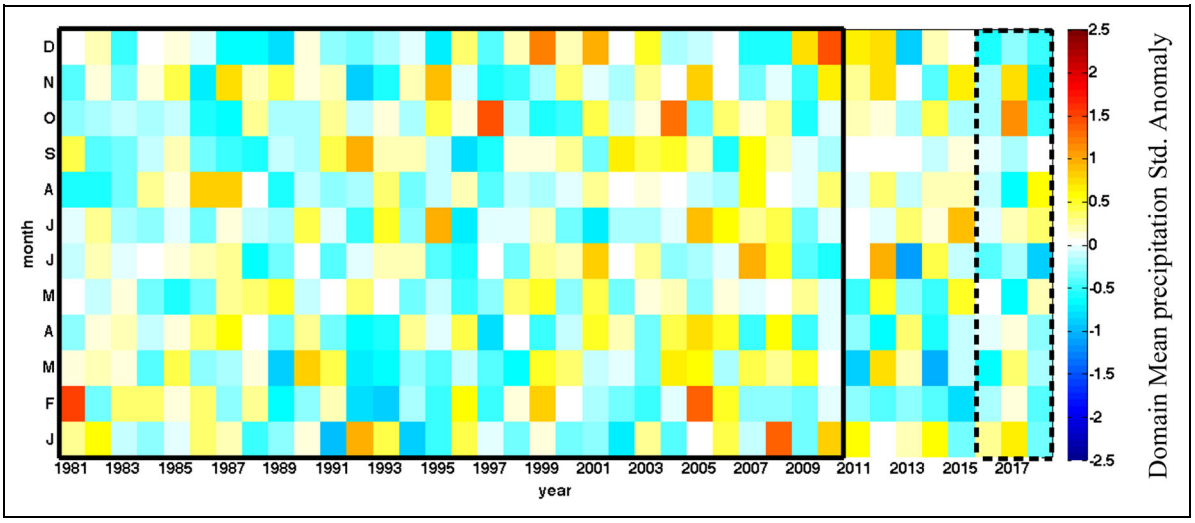

Figure 4. Monthly ERA-Interim precipitation (rainfall and snowfall) standardized anomalies from 1979 to 2018. Month–year plots of mean ERA-Interim precipitation (rainfall and snowfall) standardized anomalies spatially averaged over the Hudson Bay Complex, with red (blue) shading indicating high (low) precipitation regimes. The solid rectangle perimeter depicts the 1981–2010 climatology, and the dashed rectangle perimeter the 2016–2018 BaySys time frame. Standardized anomalies are unitless. ERA-Interim = European Centre for Medium-Range Weather Forecasts (ECMWF) Re-Analysis - Interim. DOI: https://doi.org/10.1525/elementa.2020.00126.f4

conditions in January, February, May, September, and October of 2017 (2018). In particular, positive (negative) anomalies characteristic of warm (cold) conditions are observed over southern (southern and eastern) HB in January 2017 (2018), which persist in southeastern (throughout) HB in February 2017 (2018). A southwest/northeast gradient in negative/positive anomalies is observed over (south of) HB in May 2017 (2018), resulting in predominantly negative anomalies over the HBC in the latter. Warm (cold) conditions exist over HB in September 2017 (2018), which are replaced by a northwest/southeast gradient in cold/warm conditions in October 2017, in contrast to sustained cold conditions in October 2018 (Supplemental Figures S3A–S3C). Noteworthy also in the monthly plots of surface temperature standardized anomalies is an increase in surface temperatures over the past decade, particularly during summer (June, July, August) and fall (September, October, November).

Precipitation standardized anomalies (**Figure 4**) exhibit wet (dry) conditions in January and October of 2017 (2018). In January, negative (positive) anomalies characteristic of dry (wet) conditions are observed over northern (northwest and southeast) HB in 2017, while negative anomalies are observed throughout HB in 2018. In October, all regions with the exception of southwest HB are subjected to wet conditions in 2017, in contrast to dry conditions found for 2018 (Supplemental Figures S4A–S4C). Noteworthy is the band of high precipitation in March 2017 in the vicinity of the Port of Churchill, depicting snowfall associated with the blizzard in March 2017. Monthly plots further show that less precipitation is observed in February over the past decade.

Time series reinforce similarities and differences between years for the HBC relative to the 1981–2010 climatology; uncertainty is depicted by the IQR for all area-weighted (spatially averaged) variables to highlight spatial variability within the HBC (**Figures 5**–**8**). Noteworthy are contrasting SLP high (low) regimes in October 2016 (2017) and in May 2017 (2018) as a signature of regional atmospheric circulation features. Calm (windy) conditions are evident in October 2016 (2017) and August 2017 (2018) as a signature of local (and highly variable) atmospheric contributions within the HBC. Surface temperatures exhibit less variability, although standardized anomalies show that May and August of 2017 (2018) are characterized as warm (cold) months within the HBC. Precipitation standardized anomalies show that October and November (May) are characterized as wet (dry) months in 2017, while August (June) are characterized as wet (dry) months in 2018. Spatial variability is in addition captured by confidence intervals in winds and precipitation, as is to be expected due to significant variability at local scales (Supplemental Figures S2A–S2D and S4A–S4D).

3.1.2. Terrestrial temperature, precipitation, and river discharge conditions

Terrestrial precipitation (from HydroGFD) shows a basin-wide tendency toward increased precipitation in the March to October period (**Figure 9**). Basin-wide temperature (also from HydroGFD) ranges from –25 °C in January to +15 °C in July, crossing 0 °C in March–April and October–November (**Figure 10**). Precipitation falling between October and March is largely stored as snowpack due to temperatures below freezing until warmer spring temperatures melt this snowpack leading to the nival (recession of hydrograph from October to February, freshet peak from April to June) discharge regime (modeled in H-HYPE; **Figure 11**).

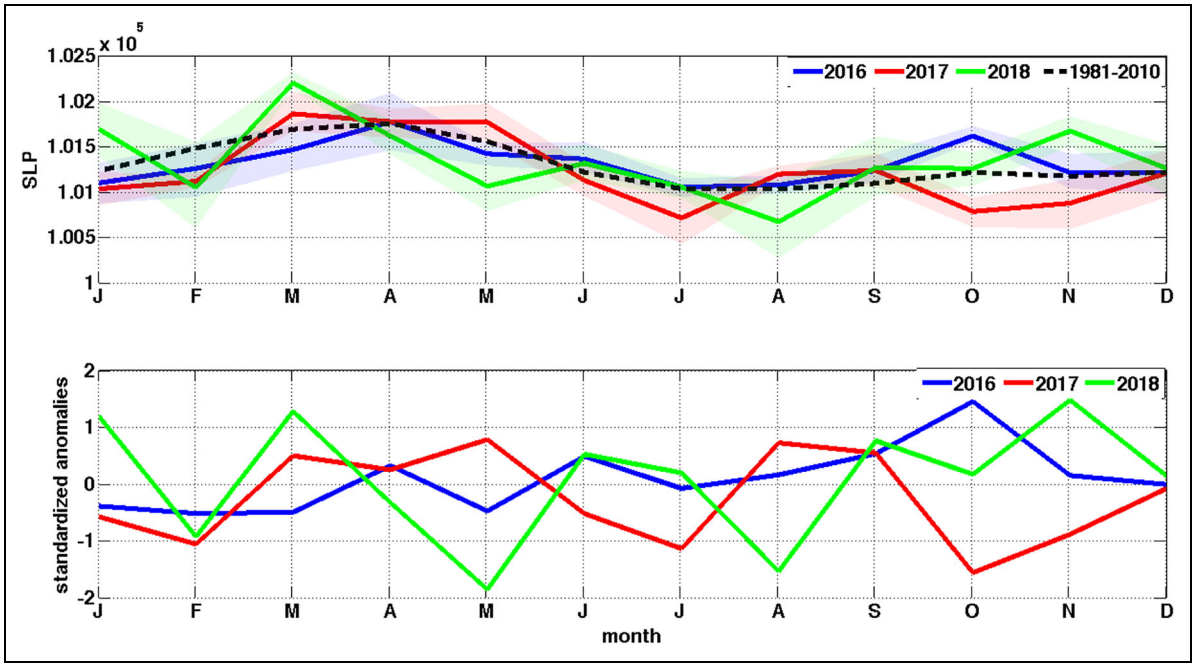

Figure 5. ERA-Interim mean sea-level pressure (SLP) and standardized anomaly time series for BaySys years relative to climatology. Monthly mean ERA-Interim SLP and standardized anomalies spatially averaged over the Hudson Bay Complex (HBC) for 2016 (blue), 2017 (red), 2018 (green), and the1981–2010 climatology (dashed black). Shading depicts the interquartile range to demonstrate spatial variability in SLP within the HBC. Mean SLP units are in [Pa], and standardized anomalies are unitless. ERA-Interim = European Centre for Medium-Range Weather Forecasts (ECMWF) Re-Analysis - Interim. DOI: https://doi.org/10.1525/elementa.2020.00126.f5

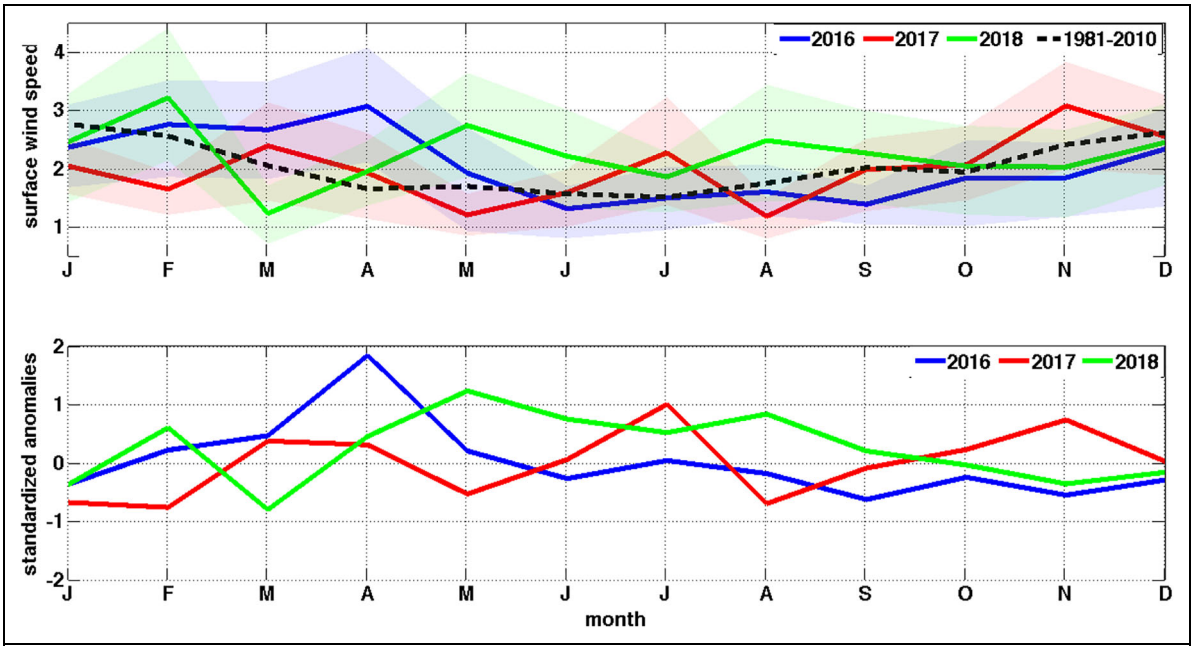

Figure 6. ERA-Interim mean wind speed and standardized anomaly time series for BaySys years relative to climatology. Monthly mean ERA-Interim wind speeds and standardized anomalies spatially averaged over the Hudson Bay Complex (HBC) for the 2016–2018 BaySys time frame relative to the 1981–2010 climatology. Shading depicts the interquartile range associated with, and spatial variability within, the spatial domain and region of interest, namely the HBC.Wind speed is in units of [m/s] and standardized anomalies are unitless. ERA-Interim = European Centre for Medium-Range Weather Forecasts (ECMWF) Re-Analysis - Interim. DOI: https://doi.org/10.1525/elementa.2020.00126.f6

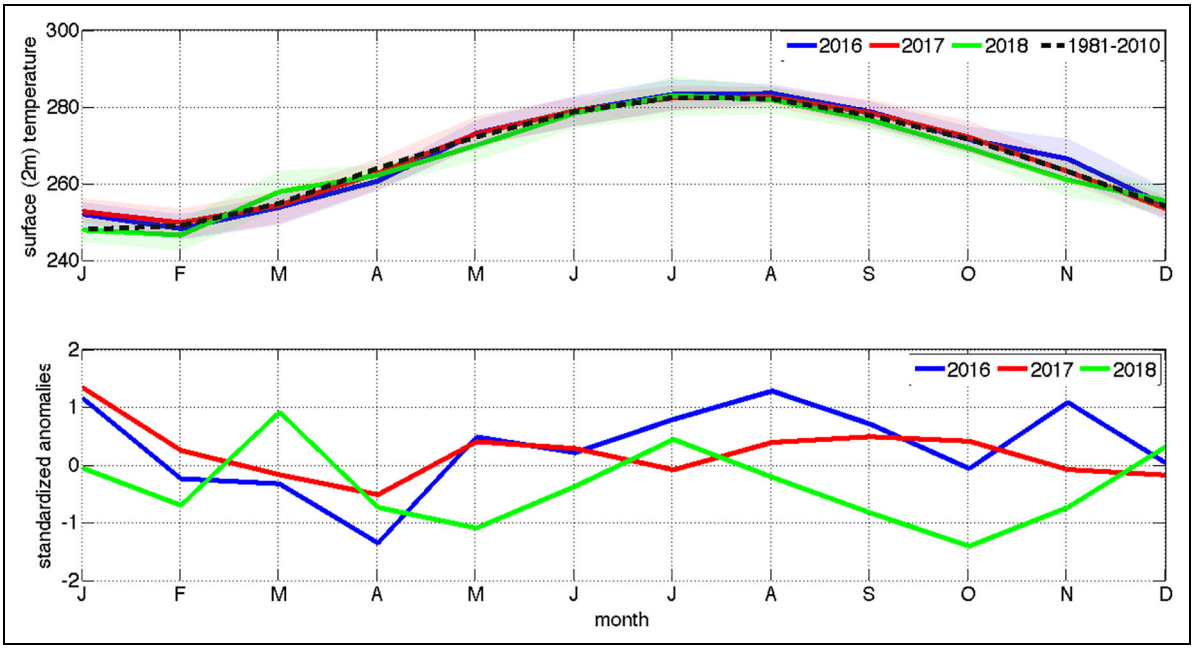

Figure 7. ERA-Interim mean surface temperature and standardized anomaly time series for BaySys years relative to climatology. Monthly mean ERA-Interim surface temperature and standardized anomalies spatially averaged over the Hudson Bay Complex (HBC), for 2016, 2017, and 2018 and the 1981–2010 climatology. Shading depicts the interquartile range associated with the HBC spatial domain and region of interest for each year. Surface temperature is in units of [K] and standardized anomalies are unitless. ERA-Interim = European Centre for Medium-Range Weather Forecasts (ECMWF) Re-Analysis - Interim. DOI: https://doi.org/10.1525/elementa.2020.00126.f7

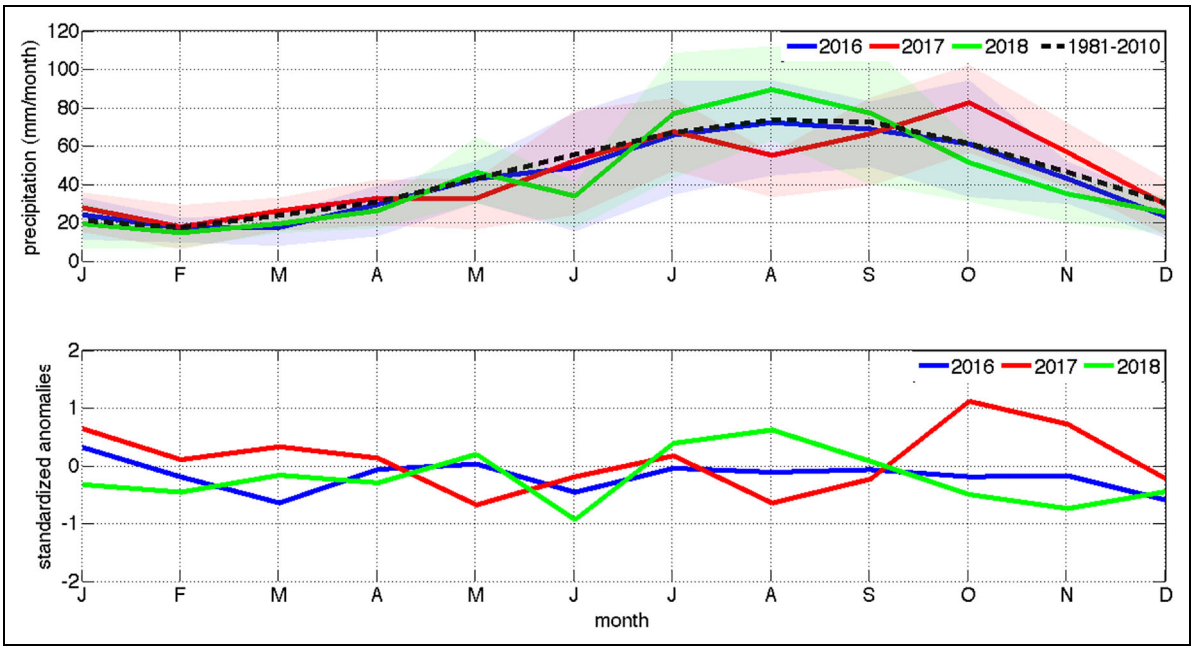

Figure 8. Mean precipitation and standardized anomaly time series for 2016, 2017, 2018 relative to 1981–2010. Monthly mean ERA-Interim precipitation and standardized anomalies spatially averaged over the HBC for 2016, 2017, 2018, and the 1981–2010 climatology. Shading depicts the interquartile range associated with the HBC spatial domain and region of interest for each year. Precipitation is in units of [mm/month] and standardized anomalies are unitless. ERA-Interim = European Centre for Medium-Range Weather Forecasts (ECMWF) Re-Analysis - Interim. DOI: https://doi.org/10.1525/elementa.2020.00126.f8

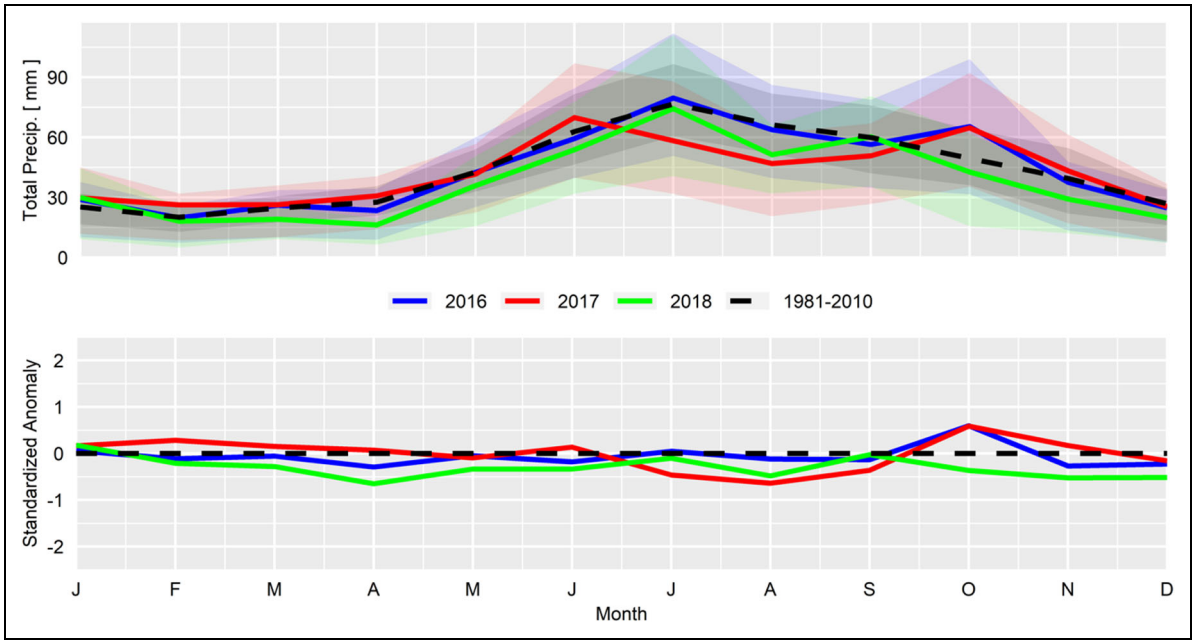

Figure 9. HydroGFDv2 mean overland precipitation and standardized anomaly time series for BaySys years relative to climatology. Monthly mean 2016 (blue), 2017 (red), and 2018 (green) HydroGFDv2 overland precipitation [mm] and standardized anomalies [unitless] relative to 1981–2010 climatology (black), spatially averaged over the Hudson Bay watershed. Shading depicts the interquartile range based on 25th and 75th percentiles for the 1981–2010 climatology. DOI: https://doi.org/10.1525/elementa.2020.00126.f9

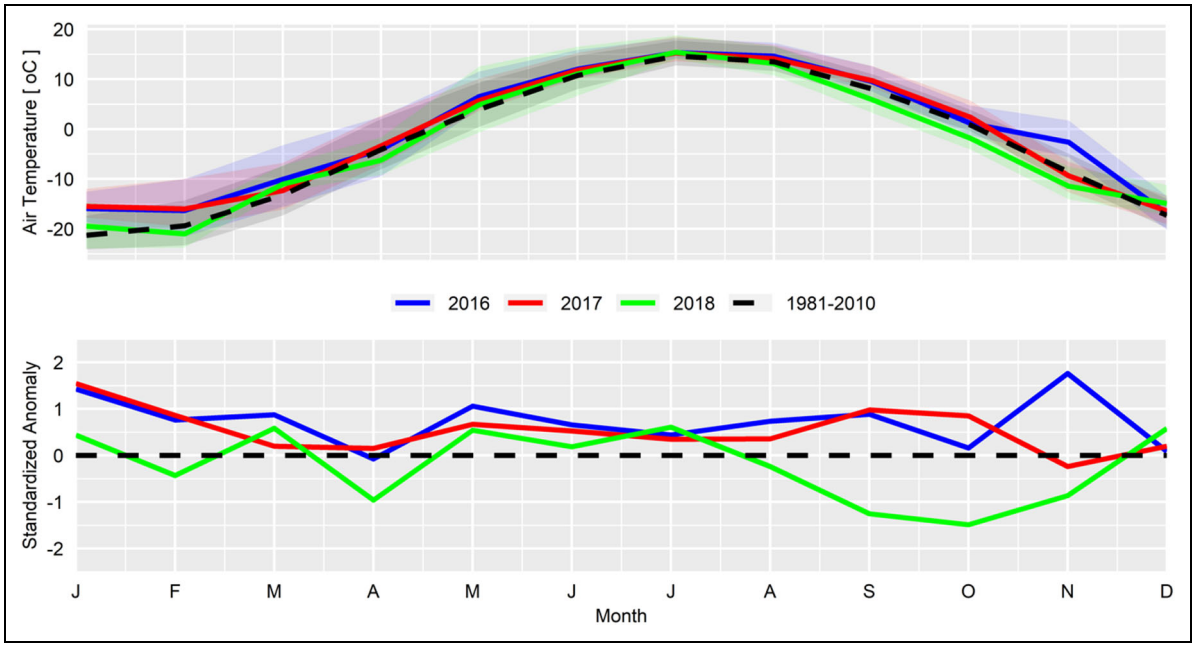

Figure 10. HydroGFDv2 mean overland temperature and standardized anomaly time series for BaySys years relative to climatology. Monthly mean 2016, 2017, and 2018 HydroGFDv2 air temperature [°C] and standardized anomalies [unitless; –] relative to 1981–2010, spatially averaged over the Hudson Bay watershed. Shading depicts the interquartile range for the 1981–2010 climatology and historical baseline time frame. DOI: https://doi.org/10.1525/elementa.2020.00126.f10

Precipitation presents a mixed record of anomalies in the observation period of 2016–2018. 2016 and 2017 both present strongly wet Octobers, with 2017 and 2018 July and August months noticeably drier than average (**Figure 12**). Standard deviation of precipitation in the baseline period 1981–2010 shows lower variance in the eastern HBW (Québec) in all months, with localized areas of higher variability over the Hudson Bay Lowlands (western James Bay and northwestern Ontario) and especially in the northwestern HB (affecting the Thelon, Kazan, Tha-

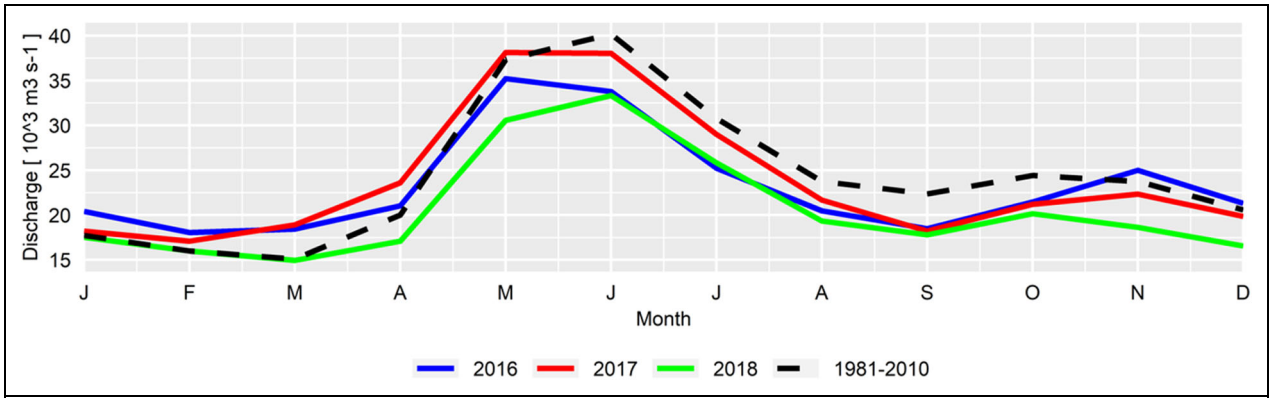

Figure 11. HYdrological Predictions for the Environment mean monthly discharge time series for BaySys years (2016, 2017, 2018) and climatology (1981–2010). Monthly mean 2016, 2017, and 2018 mean HYPE (regulated) discharge [m^3s^{-1}], sum of outlets from Hudson Bay watershed. Shading depicts the interquartile range for the 1981–2010 climatology within the physical watershed. DOI: https://doi.org/10.1525/elementa.2020.00126.f11

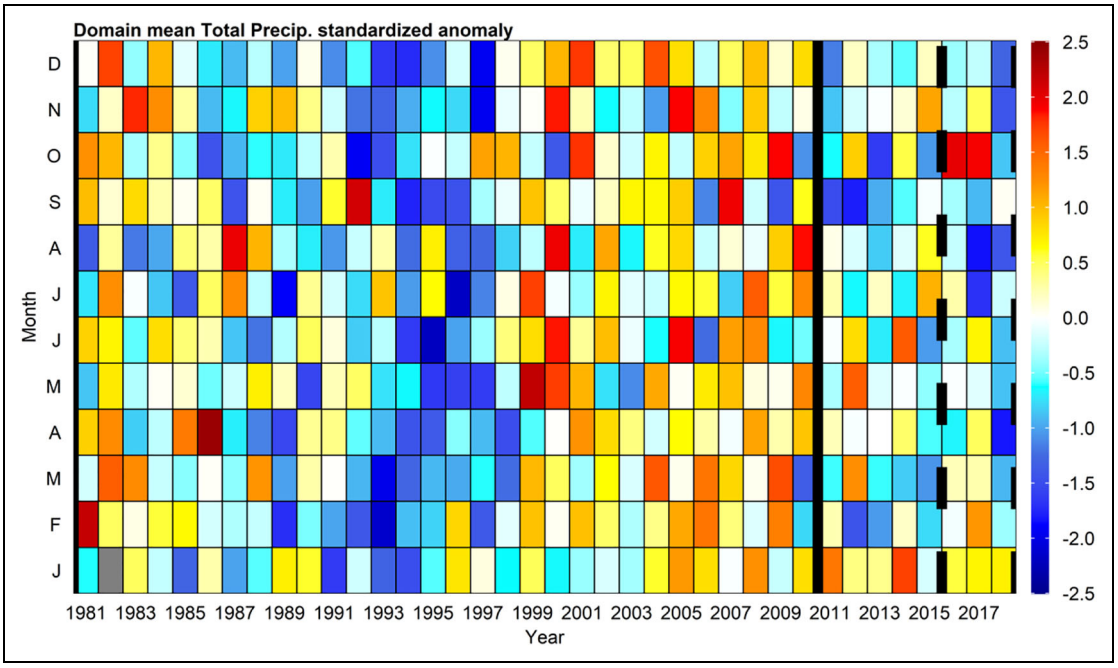

Figure 12. Monthly Hydrological Global Forcing Data (HydroGFDv2) overland precipitation standardized anomalies from 1979 to 2018. Monthly HydroGFDv2 terrestrial (overland) precipitation standardized anomalies for 1981–2018, spatially averaged over the Hudson Bay watershed, where red/blue contour shading indicates wet/dry conditions in the drainage basin. Reference period (1981–2010) outlined in solid, BaySys observation period (2016–2018) outlined in dashed. Standardized anomalies are unitless. DOI: https://doi.org/10.1525/elementa.2020.00126.f12

Anne, and Thlewiaza watersheds) and hot spots of precipitation variability over the Canadian prairies in summer, when they are subject to convective storms (Supplemental Figure S5D). In 2016, 2017, and 2018, localized precipitation is strongly anomalously wet (anomaly greater than 3σ) in the western half of the watershed in October, March and October, and January respectively (Supplemental Figures S5A, S5B, S5C). Conversely, the eastern portion of the watershed (La Grande, Koksoak, Eastmain Rivers) shows regional anomalies between −1 and +1 in all 3 years for most months.

Overland temperature in the observation period shows a positive anomaly in the majority of months for 2016 and 2017, with a warm summer and spring, cool autumn, and mixed winter (**Figure 13**). The spatial IQR of temperature is narrower relative to that of precipitation (**Figures 9** and **10**). Spatially averaged anomalies of temperature show 2016 being above or equal to the baseline period in all months except November, while 2018 presents a mixed anomaly record with a sustained cool autumn (**Figure 10**). As with the strongly seasonal and spatial temperature regime, standard deviations of temperature are greatest in summer, when temperature is greatest (Supplemental Figure S6D). Notably, greater anomalies of temperature in all months occur in the northern parts of the basin (those with lowest mean temperature), reflecting the

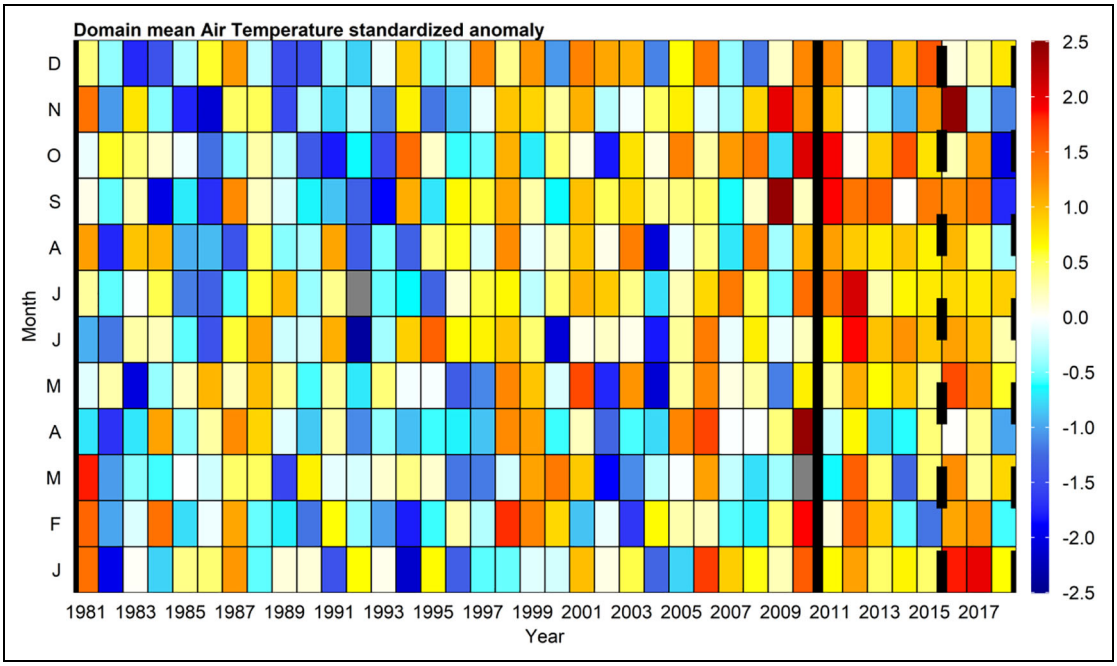

Figure 13. Monthly Hydrological Global Forcing Data (HydroGFDv2) overland temperature standardized anomalies from 1979 to 2018. Monthly HydroGFDv2 terrestrial (overland) air temperature standardized anomalies for 1981–2018, spatially averaged over the Hudson Bay watershed, where red/blue contour shading indicates warm/cool conditions in the drainage basin. Standardized anomalies are unitless. DOI: https://doi.org/10.1525/elementa.2020.00126.f13

temperatures of higher latitudes increasing at greater speeds than their southern counterparts, producing increased variance in the reference period in the northern Foxe Basin region. Spatial overland temperature anomalies show a basin-wide warm year in 2016 in all months except April, with a sustained hot spell (anomaly greater than 3σ) in the northwestern corner of the watershed (Supplemental Figure S6A), which persists until August of 2017, with the rest of the basin showing middling to warm anomalies in the rest of watershed in 2017 (Supplemental Figure S6B). 2018 temperature anomalies present a consistent cool period in autumn, with a warm to cool gradient switching from east to west in March, to northeast to southwest in April, reversing to southwest to northeast in May and June, moving again to south to north in July (Supplemental Figure S6C).

Discharge anomalies present a clearer, roughly decadal regime change (**Figure 14**). This presents itself in net discharge to the HBC as very dry in the 1990s, very wet in the 2000s, and somewhat dry in the 2010s, including the observation period 2016–2018. Examining the annual and reference time series, we see that 2016 is a wet winter and then drier than the reference period, 2017 is wetter than reference in the winter and spring, followed by dry summer and autumn, and 2018 is average or drier than average in all months (**Figure 14**). Note that as the discharge is computed as a basin net discharge, there is no spatial IQR presented. For the obvious reason of producing greater discharge, standard deviation of flow is greatest along the main river trunks (Supplemental Figure S7D). Intra-annual timing of the greatest variability presents differences river to river, with unregulated or run-of-the-river regulated rivers showing the highest variability between May and July (southern James Bay, northwestern Hudson Bay), the Nelson River's greatest reference period variability in both May and September, and the La Grande River's greatest variability in February. This is an example of the effects of regulation on the timing and variability of discharge to the HBC (Supplemental Figure S7A). Spatial anomalies of discharge present a consistent wet year in the western HBW and periodic (January and February, November and December) dry periods in the eastern HBW (Supplemental Figure S7B). The southwestern HBW produces extremely high subbasin discharge from January to June in 2017 (Supplemental Figure S7B), with the James Bay drainage (southern HBW) producing very high winter discharge in 2018, before a very wet fall in the southwestern HBW (Supplemental Figure S7C).

3.2. Rankings and extreme atmospheric and discharge conditions

The ranking in atmospheric variables SLP, surface winds, surface temperature, and precipitation spatially averaged over the HBC over the 1981–2018 time frame (**Figures 15** and **16**) highlights whether a particular month or season during the BaySys baseline 2016–2018 time frame is characterized by extreme atmospheric conditions relative to the 1981–2010 time frame. Both figures provide a synopsis of the monthly plots shown in the previous section.

Results suggest that 2016 is characterized by warm conditions throughout the annual cycle, with intervals of strong winds in spring (March, April, and May), and a dominant SLP high in September and October (**Figure 15**). In 2017, the HBC is characterized by predominantly

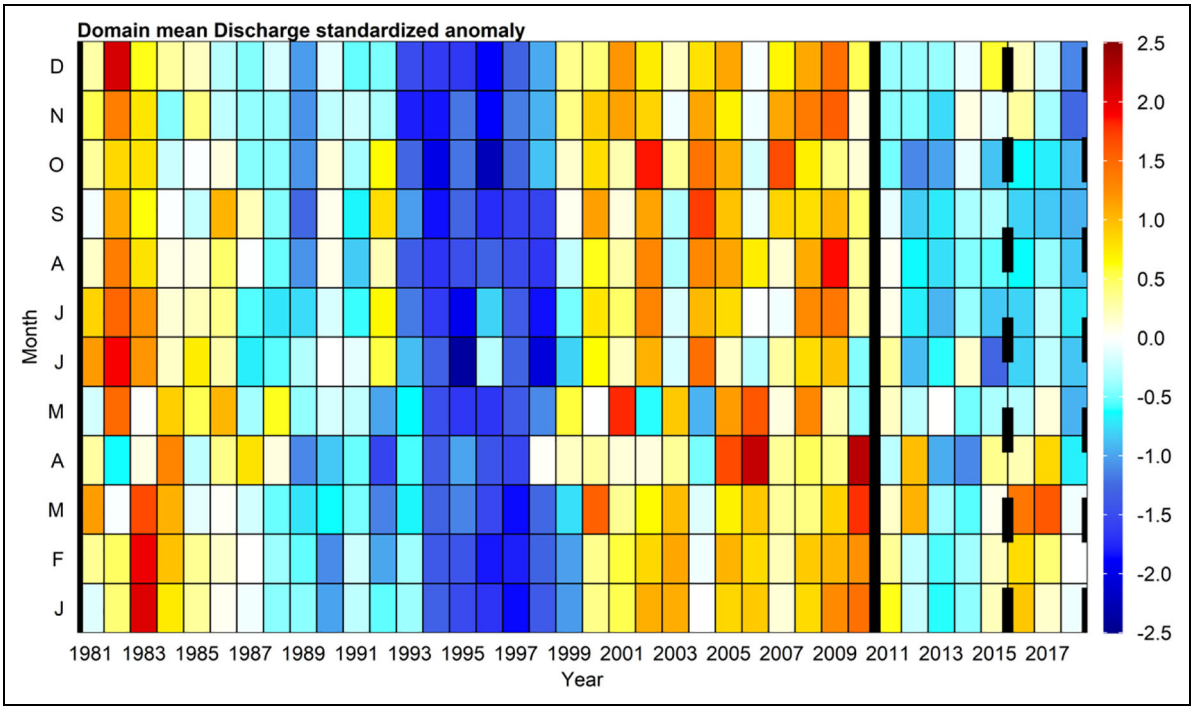

Figure 14. Monthly HYdrological Predictions for the Environment (HYPE) river discharge standardized anomalies from 1979 to 2018. Monthly mean HYPE (regulated) river discharge [$m^3;s^{-1};$] and standardized anomalies [unitless] for 1981–2018, sum of all outlets from Hudson Bay watershed, where red/blue contour shading indicates high/low discharge conditions in the drainage basin. DOI: https://doi.org/10.1525/elementa.2020.00126.f14

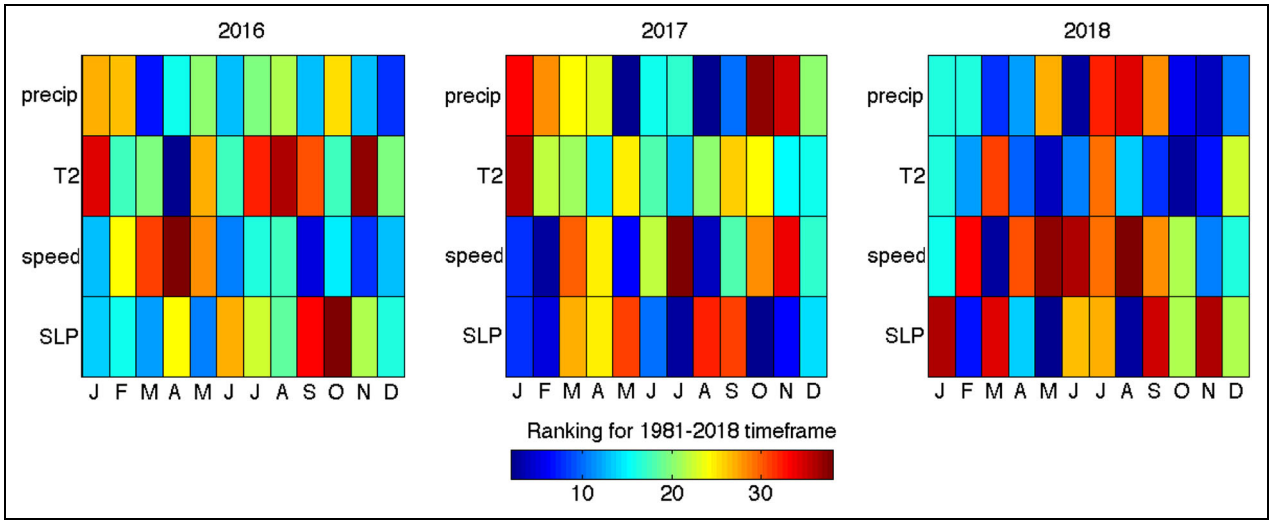

Figure 15. Rankings in sea-level pressure (SLP), wind speed, temperature, and precipitation during BaySys years for the 1981–2018 time frame. Monthly rankings for ERA-Interim atmospheric variables (SLP, surface wind speed, surface temperature, and precipitation) from 2016–2018 relative to the 1981–2018 time frame. Variables are ranked in ascending order so that low (high) values indicate comparatively low (high) regimes. ERA-Interim = European Centre for Medium-Range Weather Forecasts (ECMWF) Re-Analysis - Interim. DOI: https://doi.org/10.1525/elementa.2020.00126.f15

calm conditions, with the exception of July and November, as well as wet/high precipitation conditions in January, October, November, and an SLP high (low) regime in August and September (October and November). In 2018, cold and windy conditions are observed throughout the annual cycle, with predominantly dry conditions in winter (December, January, and February and spring (March, April, and May), wet conditions in summer; July and August), with alternating SLP regimes in winter. Extreme atmospheric conditions, defined as those for which values lie outside the upper and lower quartiles (75th and 25th percentiles) (**Figure 16**), highlight relative contributions on monthly timescales

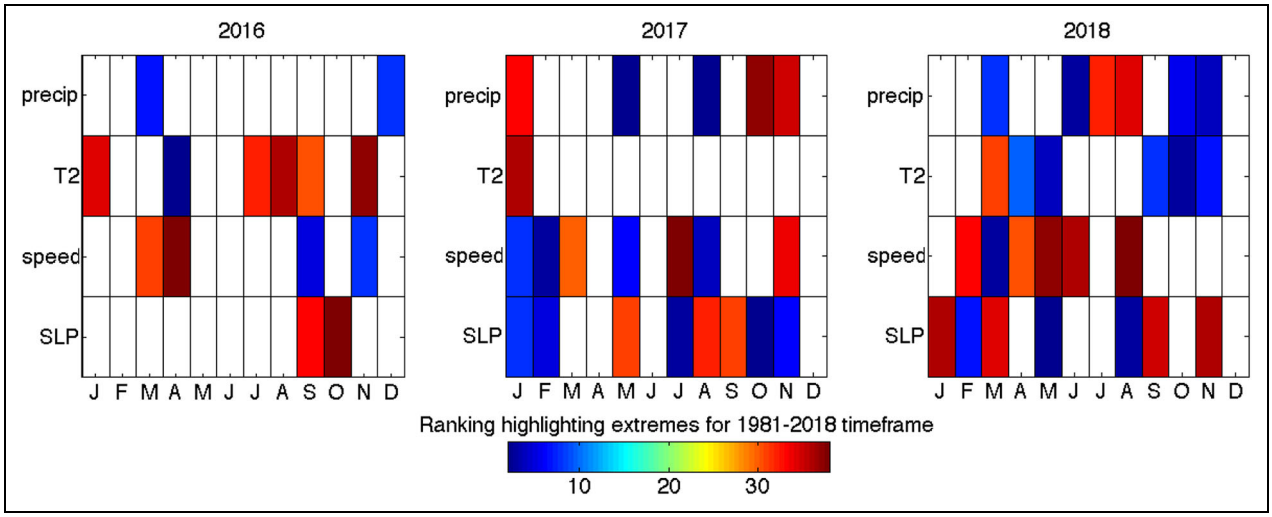

Figure 16. Rankings in atmospheric variables highlighting monthly extremes in BaySys years for the 1981–2018 time frame. Monthly rankings for ERA-Interim atmospheric variables from 2016 to 2018, showing values that lie outside of the upper and lower quartiles (75th and 25th percentiles) as an indication of extreme (i.e., sea-level pressure low/high, calm/windy, cool/warm, and dry/wet) conditions for the 1981–2018 time interval. ERA-Interim = European Centre for Medium-Range Weather Forecasts (ECMWF) Re-Analysis - Interim. DOI: https://doi.org/10.1525/elementa.2020.00126.f16

during the 2016–2018 BaySys time frame from the perspective of SLP high (low) regimes, windy (calm) conditions, warm (cold), and wet (dry) conditions; this figure provides an indication of atmospheric extremes and anomalous conditions for the 2016–2018 BaySys time frame during the 1981–2018 time interval.

The ranking in overland variables total precipitation, air temperature, and river discharge spatially averaged over the HB physical watershed for the 1981–2018 time frame (Supplemental Figures S8 and S9) highlights whether a particular month or season during the BaySys baseline 2016–2018 time frame is characterized by extreme overland and discharge conditions relative to the 1981–2010 time frame. Specifically, HydroGFD (Supplemental Figure S8) and ERA-Interim (Supplemental Figure S10) precipitation and temperature rankings are comparable, while March 2016 and 2017 depict unusually high river discharge.

3.3. Atmospheric conditions in the HBW

Time series and monthly plots for the HBW indicate departures from local phenomena in the HBC, particularly during transition seasons (Supplemental Figures S12–S19). Differences may be attributed to the location of the SLP high/low regime relative to the HBC, as well as differences in surface wind, surface temperature, and precipitation patterns outside of the HBC. As an example, lower SLP standardized anomalies for the HBW relative to the HBC in February 2017 reflect westward displacement of the SLP low (Supplemental Figure S1B). Persistence in and comparable extreme rankings for the HBW (Supplemental Figure S11) and HBC (**Figure 16**) highlight extremes due to nonlocal phenomena manifested at marine and watershed scales. Specifically, comparable SLP high (low) extreme rankings in January, March, and September (February, May, and August) and sustained correspondence between HBC and HBW extreme rankings for speed, temperature, and precipitation indicate the influence of predominantly nonlocal phenomena in 2018 in the HBC. Comparable SLP low extreme rankings for the HBC and HBW in February, July, and October in 2017 are also characteristic of nonlocal contributions to HBC processes. Differences between HBW and HBC rankings indicate differences in extremes associated with local phenomena, including blizzards, differences in sea ice cover over the HBC in winter and spring, or land/sea contrasts due to enhanced thermal temperature gradients during transition seasons. For example, rankings capture windy conditions in the HBC and high precipitation in the HBW in March 2017 characteristic of the blizzard near the Port of Churchill, where winds exceeding 120 km/h and precipitation exceeding 60 cm were reported at that time (Canadian Broadcasting Corporation News, 2017). In 2016, the absence of comparable variable extreme rankings between the HBC and HBW suggests processes are governed by local phenomena.

4. Synopsis

Results from an assessment of atmospheric and river discharge conditions in 2016, 2017, and 2018 relative to the 1981–2010 climatology highlight spatiotemporal differences between years. In particular, 2016 is characterized by warm conditions (terrestrial and marine) throughout the annual cycle, high wind speeds in spring (March and April), and high SLP in fall (September and October). In addition, 2017 is characterized by minimum SLP in January and February, SLP reversals in fall (September and October), strong winds in March in keeping with the blizzard, as well as high precipitation in January, October, and November. In 2018, cold and windy conditions predominate throughout the annual cycle. Evaluation of terrestrial

conditions show higher than normal temperatures over land (the physical HBW) in January and February, 2016 and 2017, higher than normal precipitation over land in February in 2017, and higher than normal river discharge reaching the HBC in March in 2016 and 2017. Comparable rankings for the HBC and HBW in 2018 and to a lesser extent 2017 highlight the manifestation of nonlocal atmospheric phenomena at local and regional scales. Differences in the HBC and HBW extreme rankings capture local extreme events such as blizzards, evident in particular in windy conditions in the HBC and high precipitation in the HBW in March 2017 characteristic of the March 7-9, 2017, blizzard.

This article presents a framework for the spatiotemporal evaluation of atmospheric and river discharge conditions in the HBC, as "input" to the ANHA configuration of the NEMO model. Rankings relative to the 1981–2010 climatology provide an index for extreme events, on monthly timescales, in atmospheric and discharge conditions that are useful for providing context for analyses of observations collected during the BaySys 2016–2018 field campaign observations. A similar analysis as presented here is conducted by Lukovich et al. (n.d.) for ice and oceanographic conditions which, from the perspective of modeling, serve as the "output" from the ANHA configuration of the NEMO model and the BaySys project. Implications of extreme atmospheric and river discharge conditions on physical and biogeochemical processes during the BaySys time frame will be explored in future studies. These implications will aid the development of additional diagnostics and indices relevant for communities from the perspective of planning and preparedness.

Data accessibility statement

The ERA-Interim atmospheric forcing data set (Dee et al., 2011) and variables used in this study (SLP, zonal and meridional surface winds, surface temperature, and precipitation) were downloaded from https://www.ecmwf.int/en/forecasts/datasets/reanalysis-datasets/era-interim.

HydroGFDv2 terrestrial (overland) temperature and precipitation data (Berg et al., 2018) can be obtained from *Climate Impacts* at https://hypeweb.smhi.se/explore-water/climate-change-data/global-climate-change/.

Modeled discharge data from the Arctic HYPE (AHYPE; Andersson et al., 2015) hydrological model are published online at https://hypeweb.smhi.se/explore-water/model-performances/model-performance-arctic/, while modeled discharge data used in the present study from a configuration of the AHYPE hydrological model, the H-HYPE (regulated) model, are made available through the BaySys data repository (open access).

Supplemental files

The supplemental files for this article can be found as follows:

Figures S1–19. Equations. Table of Acronyms. PDF

Acknowledgments

This work is a contribution to the Natural Sciences and Engineering Council of Canada Collaborative Research and Development project titled BaySys. In addition, this research contributes to the ArcticNet Networks of Centers of Excellence and the Arctic Science Partnership. The authors would also like to thank the Elementa Atmospheric Science Associate Editor, Dr. Erika von Schneidemesser, Editor in Chief, Dr. Detlev Helmig, and two anonymous reviewers for constructive suggestions.

Funding

Funding for this research was graciously provided by Manitoba Hydro, NSERC, Amundsen Science, and the Canada Research Chairs program.

Competing interests

The authors declare no competing interests.

Author contributions

Contributed to conception and design: JVL, AT, KS.

Contributed to acquisition of data: AT, SJ, CP, PGM, TAS.

Contributed to analysis and interpretation of data: JVL, AT.

Drafted and/or revised the article: JVL, AT, SJ, PGM, JCS, KS, KW, MV, TAS.

Approved the submitted version for publication: All authors.

References

Andersson, A, Meier, HEM, Ripszam, M, Rowe, O, Wikner, J, Haglund, P, Eilola, K, Legrand, C, Figueroa, D, Paczkowska, J, Lindehoff, E, Tysklind, M, Elmgren, R. 2015. Projected future climate change and Baltic Sea ecosystem management. *AMBIO* **44**: 345–356. DOI: http://dx.doi.org/10.1007/s13280-015-0654-8.

Berg, P, Donnelly, C, Gustafsson, D. 2018. Near-real-time adjusted reanalysis forcing data for hydrology. *Hydrology and Earth System Sciences* **22**: 989–1000. DOI: http://dx.doi.org/10.5194/hess-22-989-2018.

Canadian Broadcasting Corporation News. 2017, March 12. Churchill declares state of local emergency after three days of blizzard. Available at https://www.cbc.ca/news/canada/manitoba/manitoba-churchill-blizzard-emergency-1.4020872.

Cavallo, SM, Hakim, GJ. 2010. Composite structure of tropopause polar cyclones. *Monthly Weather Review* **138:** 3840–3857. DOI: http://dx.doi.org/10.1175/2010mwr3371.1.

Crawford, AD, Serreze, MC. 2016. Does the summer Arctic Frontal Zone influence Arctic Ocean cyclone activity? *Journal of Climate* **29**: 4977–4993. DOI: http://dx.doi.org/10.1175/JCLI-D-15-0755.1.

Dabernig, M, Mayr, GJ, Messner, JW, Zeileis, A. 2017. Spatial ensemble post-processing with standardized anomalies. *Quarterly Journal of the Royal Meteorological Society* **143**: 909–916. DOI: http://dx.doi.org/10.1002/qj.2975.

Dee, DP, Uppala, SM, Simmons, AJ, Berrisford, P, Poli, P, Kobayashi, S, Andrae, U, Balmaseda, MA, Balsamo, G, Bauer, DP, Bechtold, P. 2011. The ERA-interim reanalysis: Configuration and performance

of the data assimilation system. *Quarterly Journal of the Royal Meteorological Society* **137**: 553–597. DOI: http://dx.doi.org/10.1002/ qj.828.

Déry, SJ, Mlynowski, TJ, Hernandez-Henriquez, MA, Straneo, F. 2011. Interannual variability and interdecadal trends in Hudson Bay streamflow. *Journal Marine Systems* 88: 341–351.

Déry, SJ, Stadnyk, TA, MacDonald, MK, Gauli-Sharma, B. 2016. Recent trends and variability in river discharge across northern Canada. *Hydrology and Earth System Sciences* **20**(12): 4801–4818. DOI: http://dx.doi.org/10.5194/hess-20-4801-2016.

Déry, SJ, Stadnyk, TA, MacDonald, MK, Koenig, KA, Guay, C. 2018: Flow alteration impacts on Hudson Bay river discharge. *Hydrological Processes* **32**: 3576–3587. DOI: http://dx.doi.org/10.1002/hyp.13285.

Dmitrenko, IA, Myers, PG, Kirillov, SA, Babb, DG, Volkov, DL, Lukovich, JV, Tao, R, Ehn, JK, Sydor, K, Barber, DG. 2020. Atmospheric vorticity sets the basin-scale circulation in Hudson Bay. *Elementa: Science of the Anthropocene* **8**(1): 049. DOI: https://doi.org/10.1525/elementa.049.

Gagnon, AS, Gough, WA. 2005. Trends in the dates of ice freeze-up and breakup over Hudson Bay, Canada. *Arctic* **58**(4): 370–382.

Grill, G, Lehner, B, Lumsdon, AE, MacDonald, GK, Zarfl, C, Liermann, CR. 2015. An index-based framework for assessing patterns and trends in river fragmentation and flow regulation by global dams at multiple scales. *Environmental Research Letters* **10**(1): 015001.

Hochheim, KP, Barber, DG, 2010: Atmospheric forcing of sea ice in Hudson Bay during the fall period, 1980–2005. *Journal of Geophysical Research* **115**: C05009. DOI: http://dx.doi.org/10.1029/2009JC005334.

Hochheim, K, Lukovich, JV, Barber, DG. 2011. Atmospheric forcing of sea ice in Hudson Bay during the spring season, 1980–2005. *Journal of Marine Research* **88**(3): 476–487.

Ingram, RG, Prinsenberg, S. 1998. Coastal oceanography of Hudson Bay and surrounding eastern Canadian waters, in Robinson, AR, Brink, KH eds., *The global coastal ocean*. New York, NY: John Wiley and Sons, Inc. (The sea; vol. 11): 105–133.

JafariKhasragh, S, Lukovich, JV, Hu, X, Myers, PG, Sydor, K, Barber, DG. 2019. Modelling Sea surface temperature (SST) in the Hudson Bay Complex using Bulk heat flux parameterization: Sensitivity to atmospheric forcing and model resolution. *Atmosphere-Ocean*. DOI: http://dx.doi.org/10.1080/07055900.2019.1605974.

Kirillov, S, Babb, D, Dmitrenko, I, Landy, J, Lukovich, J, Ehn, J, Sydor, K, Barber, D, Stroeve, J. 2020. Atmospheric forcing drives the winter sea ice thickness asymmetry of Hudson Bay. *Journal of Geophysical Research: Oceans* **125**. DOI: http://dx.doi.org/10.1029/2019JC015756.

Landy, JC, Ehn, JK, Babb, DG, Thériault, N, Barber, DG. 2017. 'Sea ice thickness in the Eastern Canadian Arctic: Hudson Bay Complex & Baffin Bay.' *Remote Sensing of Environment* **200**: 281–294.

Lukovich, JV, Jafarikhasragh, S, Tefs, A, Myers, PG, Sydor, M, Wong, K, Stroeve, JC, Stadnyk, TA, Babb, D, Barber, DG. n.d. A baseline evaluation of oceanographic and sea ice conditions in the Hudson Bay Complex during 2016-2018. *Elementa: Science of the Anthropocene,* in press.

Maxwell, JB, 1986. A climate overview of the Canadian Inland Seas, in Martini, EP ed., *Canadian inland seas*. New York, NY: Elsevier (Elsevier oceanography series, vol. 44): 79–99. Available at https://www.ccg-gcc.gc.ca/publications/icebreaking-deglacage/ice-navigation-glaces/page04-eng.html.

Mysak, LA, Ingram, RG, Wang, J, van der Baaren, A. 1996. The anomalous sea-ice extent in Hudson Bay, Baffin Bay and the Labrador Sea during three simultaneous NAO and ENSO episodes. *Atmosphere-Ocean* **34**(2): 313–343. DOI: http://dx.doi.org/10.1080/07055900.1996.9649567.

National Snow and Ice Data Centre Arctic Sea Ice News & Analysis, Monthly Archives. 2016, May. Available at http://nsidc.org/arcticseaicenews/2016/05/.

Prinsenberg, SJ. 1986a. Salinity and temperature distribution of Hudson Bay and James Bay, in, Martini IP ed., *Canadian inland seas*. Amsterdam, the Netherlands: Elsevier: 163–186.

Prinsenberg, SJ. 1986b. The circulation pattern and current structure of Hudson Bay, in, Martini, IP ed., *Canadian inland seas*. Amsterdam, the Netherlands: Elsevier: 187–204.

Prinsenberg, SJ. 1987. Seasonal current variations observed in western Hudson Bay. *Journal of Geophysical Research* **92**: 10,756–10,766.

Proshutinsky, A, Dukhovskoy, D, Timmermans, ML, Krishfield, R, Bamber, J. 2015. Arctic circulation regimes. *Philosophical Transactions of the Royal Society* **373**: 1–18. DOI: http://dx.doi.org/10.1098/rsta.2014.0160.

Ridenour, NA, Hu, X, Jafarikhasragh, S, Landy, JC, Lukovich, JV, Stadnyk, TA, Sydor, K, Myers, PG, Barber, DG. 2019. Sensitivity of freshwater dynamics to ocean model resolution and river discharge forcing in the Hudson Bay Complex. *Journal of Marine Systems* **196**: 48–64.

Saucier, FJ, Dionne, J. 1998. A 3-D coupled ice-ocean model applied to Hudson Bay, Canada: The seasonal cycle and time dependent climate response to atmospheric forcing and runoff. *Journal of Geophysical Research* **103**: 27689–27705.

Saucier, FJ, Senneville, S, Prinsenberg, S, Roy, F, Smith, G, Gachon, P, Caya, D, Laprise, R, 2004. Modelling the sea ice-ocean seasonal cycle in Hudson Bay, Foxe Basin and Hudson Strait, Canada. *Climate Dynamics* **23**: 303–326.

Screen, JA, 2017. Simulated atmospheric response to regional and pan-arctic sea ice loss. *Journal of Climate* **30**: 3945–3962. DOI: http://dx.doi.org/10.1175/JCLI-D-16-0197.1.

Stadnyk, TA, MacDonald, MK, Tefs, A, Déry, SJ, Koenig, K, Gustafsson, D, Isberg, K, Arheimer, B. 2020. Hydrological modeling of freshwater discharge into Hudson Bay using HYPE. *Elementa: Science of the Anthropocene* **8**(1): 43. DOI: http://doi.org/10.1525/elementa.439.

Stewart, DG, Lockhart, WL. 2005. An overview of the Hudson Bay marine ecosystem. Canadian technical report of fisheries and aquatic sciences. No. 2586. Available at http://www.dfo-mpo.gc.ca/libraries-bibliotheques/toc-tdm/314704-eng.htm.

Walsh, JE. 2014. Intensified warming of the Arctic: Causes and impacts on middle latitudes. *Global and Planetary Change* **117**: 52–63. DOI: http://dx.doi.org/10.1016/j.gloplacha.2014.03.003.

Whittaker, R. 2006. Assessment of the Potential Environmental Impact of the La Grande River Complex on Hudson Bay and the Inuit Coastal Communities in Northern Québec. GeoArctic – Makivik Report Final Version 1.1, Calgary, Alberta.

How to cite this article: Lukovich, JV, Tefs, A, Jafarikhasragh, S, Pennelly, C, Myers, PG, Stadnyk, TA, Sydor, K, Wong, K, Vieira, M, Landry, D, Stroeve, JC, Barber, DG. 2021. A baseline evaluation of atmospheric and river discharge conditions in the Hudson Bay Complex during 2016–2018. *Elementa: Science of the Anthropocene* 9(1). DOI: https://doi.org/10.1525/elementa.2020.00126

Domain Editor-in-Chief: Detlev Helmig, Boulder AIR LLC, Boulder, CO, USA

Associate Editor: Erika von Schneidemesser, Institute for Advanced Sustainability Studies, Potsdam, Germany

Knowledge Domain: Atmospheric Science

Part of an Elementa Special Feature: BaySys

Published: June 14, 2021 **Accepted:** May 17, 2021 **Submitted:** August 31, 2020

ELEMENTA Science of the Anthropocene

Elem Sci Anth is a peer-reviewed open access journal published by University of California Press.

OPEN ACCESS